

High-Na dacite from the Jean Charcot Trough (Vanuatu), Southwest Pacific

Setsuya Nakada^a, Patrick Maillet^b, Marie-Claire Monjaret^c, Akihiko Fujinawa^d and Tetsuro Urabe^e

^aDepartment of Earth and Planetary Sciences, Kyushu University, Fukuoka 812, Japan

^bORSTOM, Centre de Brest, B.P. 70, 29280 Plouzane, France

^cURA no. 1278 "Genèse et Evolution des Domaines Océaniques", Université de Bretagne Occidentale, 6 Avenue Le Gorgeu, 29287 Brest Cedex, France

^dDepartment of Earth Sciences, Ibaraki University, Mito 310, Japan

^eGeological Survey of Japan, Higashi, Tsukuba, Ibaraki 305, Japan

(Received December 28, 1992; revision accepted April 19, 1993)

ABSTRACT

Nakada, S., Maillet, P., Monjaret, M.-C., Fujinawa, A. and Urabe, T., 1994. High-Na dacite from the Jean Charcot Trough (Vanuatu), Southwest Pacific. In: J.-M. Auzende and T. Urabe (Editors), North Fiji Basin: STARMER French-Japanese Program. *Mar. Geol.*, 116: 197–213.

Rifting that produced the Jean Charcot Trough (JCT) in the Vanuatu back-arc region commenced 2–3 Ma, leading to SiO₂-bimodal magmatism in the northern half of the trough. Dacite with high Na₂O (>6.0%) and low K₂O (<1.0%) was recovered from the northern termination of the JCT, accompanied by tholeiitic N-MORB-type back-arc basin basalt similar to that erupted at the central spreading axis of the North Fiji Basin (NFB). Incompatible element ratios are very similar in the dacite and associated basalt, and also in the NFB back-arc basin basalts (Zr/Rb > 10, Nb/Rb > 0.5, Y/Rb > 2.0, Nb/La > 0.5, and Ba/Zr < 1.5), but are quite different to lavas from the active Vanuatu volcanic arc.

The dacites are compositionally close to oceanic plagiogranite produced during fractional crystallization of an N-MORB basaltic magma, and mass balance calculations show that they may be similarly derived from the associated basalts. We show that JCT basalts are derived from a mantle source compositionally very close to that beneath the central spreading axis of the NFB, with minimal contamination by a subduction component. Westward injection of diapiric source mantle similar to that of the NFB back-arc basin basalts may have caused rifting of the JCT. During incipient back-arc rifting, high Na/K felsic magmas may have evolved from parental low-K basalts via side-wall crystallization within a large lower crustal magma chamber.

Introduction

The Jean Charcot Trough (JCT) is one of the young intra-arc troughs developed at the rear of the Vanuatu (New Hebrides) arc (Monjaret et al., 1991). Recent detailed marine geophysical and geological studies of the JCT using a deep-tow camera and the submersible *Cyana* in 1989–1991 during the STARMER program (Scientific Party on Board R/V Kaiyo, 1990; Scientific Party on Board R/V Noroit, 1992) showed that recent magmatism is restricted to the northern half of the JCT. Basaltic lavas varying compositionally from back-

arc basin basalts (BABB) and basalts intermediate between MORB and island-arc tholeiites (IAT), as well as low-K dacite lavas were dredged from the northernmost part of the trough (Monjaret et al., 1991). These have geochemical signatures unlike lavas from the modern Vanuatu arc. The dredged dacite is notably enriched in Na₂O and depleted in K₂O, and is referred to as a high-Na dacite. Such dacites are rare in modern arc-back-arc basin systems, but are reported from Deception Island, developed within the Bransfield Strait, a young back-arc basin trough (Weaver et al., 1979). The petrogenesis of these high-Na, low-K dacites may

be a useful key to aid understanding of the origin of back-arc rifting. In this paper, we describe geochemical characteristics of these lavas and discuss the petrogenesis of the JCT volcanic series.

Geological setting

Vanuatu Arc

The Vanuatu Arc, more than 1000 km long, develops along the western margin of the North Fiji Basin (NFB) (Fig. 1). The Australian plate has been subducted eastward beneath the Vanuatu arc since at least the late Miocene (Macfarlane et al., 1988), and the present convergent rate varies along the arc from 9 to 15 cm/yr, with the angle of subduction being greater than 60° (Louat and Pelletier, 1989). The D'Entrecasteaux Ridge (DCR) has collided with the central part of the arc, causing complex regional stress patterns

(Roca, 1978; Collot and Fisher, 1991) and regional uplift adjacent to the collision zone. North and south from the collision zone, the regional stress pattern changes from compressional to extensional as the effect of the collision diminishes.

The oldest rocks in the Vanuatu arc are believed to be of late Oligocene age (Fig. 1; Macfarlane et al., 1988), and the modern active central chain volcanics were erupted on to upper Miocene basement since late Pliocene time. A broad SiO_2 -bimodality characterizes lavas of the Vanuatu arc (Macfarlane et al., 1988), with peaks in the basalt-basaltic andesite and dacite compositional ranges. Most basalts are tholeiitic, but high-K basalts are common in the collision zone (Gorton, 1977; Eggins, 1993; Picard et al., 1993), and calc-alkaline lavas dominate in Matthew and Hunter volcanoes at the southern end of the arc (Maillet et al., 1986; Monzier et al., 1993). In general terms, the Vanuatu arc lavas are considered to be derived by high degrees of partial melting of an N-MORB mantle source contaminated by slab-derived fluids (Dupuy et al., 1982). Barsdell et al. (1982) showed that the K_2O content of volcanic rocks decreases away from the Vanuatu trench at the northern end of the arc, opposite to the "normal" trend in arcs. They speculated that this unusual feature may record the effects of a west-dipping Miocene subduction episode.

Back-arc troughs

Two back-arc troughs are developed in both the northern and southern parts of the Vanuatu arc, just behind the active volcanic chain. These are the Jean Charcot Trough (JCT) and the Coriolis Trough (CRT), respectively (Récy et al., 1990; Monjaret et al., 1991). Earthquakes beneath the troughs occur at 150–350 km (Louat et al., 1988). The two troughs show important differences in their structure and tectonic history. Multiple, large box-like grabens characterize the CRT, with a total length of around 300 km, maximum width of 40 km, and depths from 2000 to 3000 m. K–Ar ages for rock samples dredged from the CRT range from 6 to 0.4 Ma, but no active magmatism has been found (Monjaret et al., 1991). In contrast, the JCT is characterized by repeated, discontinu-

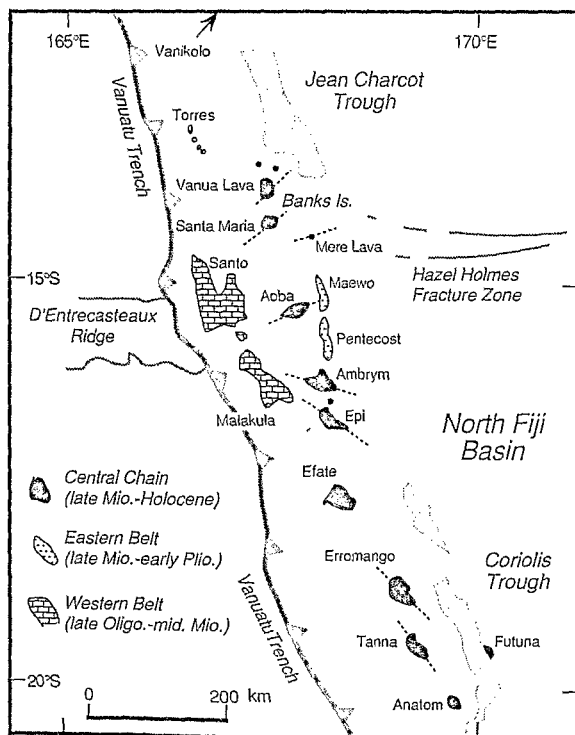


Fig. 1. Index map showing the principal geologic and tectonic features of the Vanuatu (New Hebrides) arc. Dotted lines represent the axes of horizontally maximum stress estimated from vent alignments of volcanic islands. Modified from Macfarlane et al. (1988).

ous, N-S trending horsts and grabens from 5 to 20 km width. The total width of the trough is about 60 km and it is at least 150 km long; it is mainly 1500–2000 m deep, but may deepen to more than 3000 m in places. The northern limit is near the active volcano of Vanikolo Island (just north of Fig. 1). An intra-arc sedimentary basin extended west of the JCT (Monjaret et al., 1991).

Compositional characteristics of the JCT and CRT volcanics are summarized by Monjaret et al. (1991). Most are tholeiitic, and some are enriched in alkalis (Monjaret, 1989; Monjaret et al., 1991). Rocks from the southern end of the JCT are typically arc-like, and similar to those of the active Vanuatu arc. In contrast, those from the northern end of the JCT are more typically back-arc basin basalts, varying from MORB-like, to basalts intermediate between MORB and island-arc tholeiites (IAT); also recovered were low-K dacites. Some of the JCT volcanics reported by Monjaret et al. (1991) are from inactive parts of the trough, and are probably from the basement of the Vanuatu arc in this region.

Jean Charcot Trough

Seabeam and seismic surveys during the SEAPSO and KAIYO 89 cruises (Récy et al., 1990; Scientific Party on Board R/V Kaiyo, 1990) showed relatively young volcanic cones built on the floor of the north-central parts of the JCT, and horsts bounded by high-angle fault scarps in the southern part. A typical cross-section of the JCT, based on seismic data, is shown in Fig. 2. A methane anomaly was found at Station 31 (12°12.5'S, 167°38.8'E) in the northernmost end of the JCT, and heat flow measurement via a piston core recorded the highest values (161 mW/m²) at 3027 m of water in a narrow graben at Station 40 (12°46.0'S, 167°49.5'E). A large twin-peaked volcano is situated in the northern part of the trough (Stations 31 and 33), and was dredged during SEAPSO 2 and was the focus of a deep-tow camera survey during KAIYO 89. The *Cyana* submersible carried out a detailed survey in the central and southern parts of the JCT during the SAVANES 91–92 cruise (Scientific Party on Board R/V Le Noroit, 1992).

Near Station 41 in the central part of the JCT,

two volcanoes, the western one andesitic, the eastern one basaltic, were surveyed by the *Cyana* and shown to be cut by common near N-S-trending active faults. Hydrothermal alteration was observed in the western volcano, which is about 11 km across and 1200 m high (dives no. 1140 and 1141). Debris-flow deposits are widely distributed on the flanks of the volcano, and a dike swarm was also observed, along with abundant quenched andesitic blocks usually less than 30 cm across. The eastern volcano (~12°33'S, 167°48'E) is about 15 km across, ~1400 m high, with gentler slopes than the western cone, and is characterized by piling of pillow lobes, sheet-like flows and hyaloclastites (dives no. 1142 and 1143). Some feeder dikes also crop out, and close-packed pillows are exposed on fault scarps. Lavas recovered from these cones are commonly coated by Mn usually less than a few millimeters thick. A community of sea-plants (deep-sea corals and algae) and animals (galatheas, sponges and shrimps) was observed on one summit peak (1425 m depth), together with a faint positive temperature anomaly, suggesting a possible hydrothermal environment, and supporting the existence of active magmatism in the northern JCT.

A submersible survey of the western margin of the central part of the JCT (dive no. 1144; west of Station 41 at ~12°39'S, 167°33'E) showed no evidence of recent tectonic or volcanic activity, thick Mn-coatings on rounded rocks, and slopes shallower than 1900 m covered with thick sediments. Rocks recovered are altered intrusives, probably associated with basement rocks of the central chain volcanoes.

In contrast, seamounts with morphology suggesting recent volcanic activity have not been found in the southern half of the JCT (Stations 39 and 42). Submersible and deep-tow camera surveys (Scientific Party on Board R/V Kaiyo, 1990; Scientific Party on Board R/V Le Noroit, 1992) show layers of volcanoclastic rocks and rare lavas exposed only on steep cliffs (probably fault scarps).

Samples recovered from the JCT during the SEAPSO 2 and STARMER cruises, mostly volcanics, include rocks with K–Ar ages > 4.5 Ma (Monjaret et al., 1991). However, those taken from the volcanic cones (Stations 31 and 41) have K–Ar ages

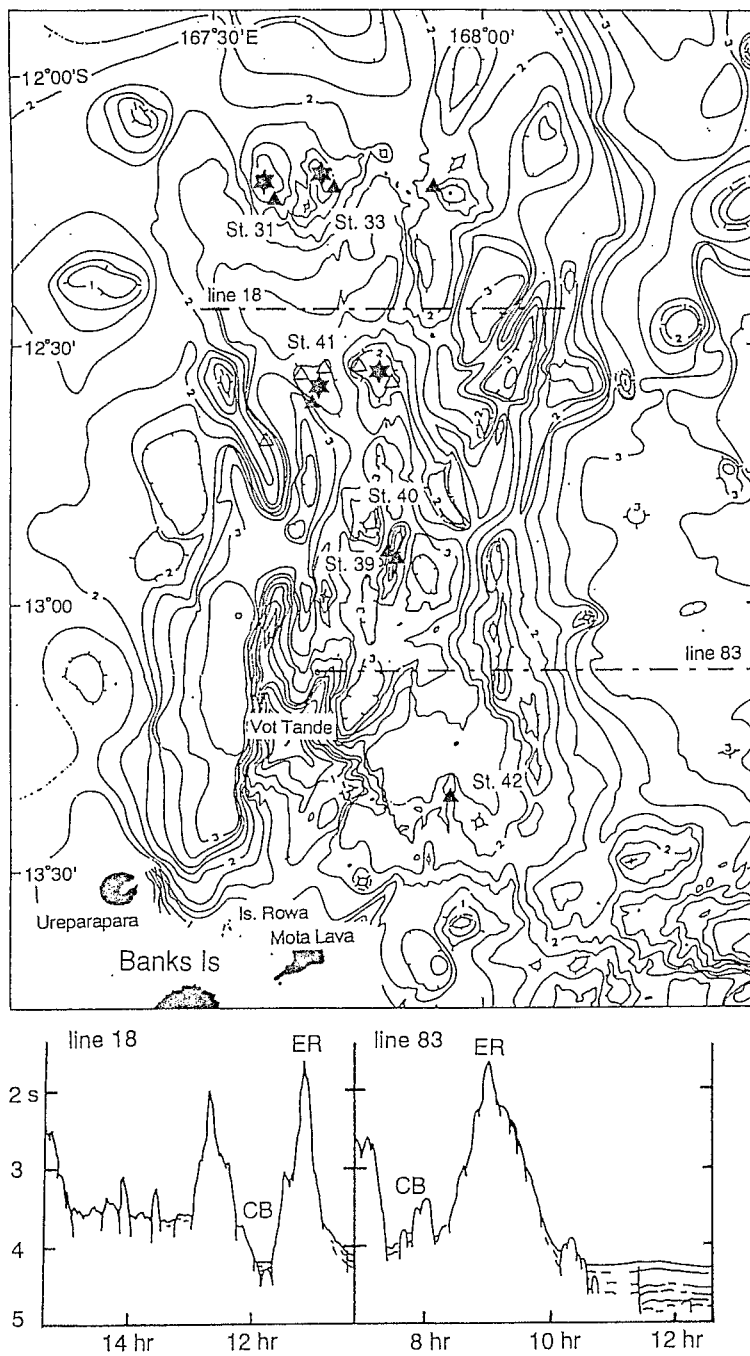


Fig. 2. Bathymetric map of the Jean Charcot Trough (after Charvis and Pelletier, 1989), showing positions of volcanic cones (stars) and sample localities (solid and open triangles = dredge and dive sites, respectively) in STARMER cruises (KAIYO 89 and SAVANES 91-92). Contour lines with 250 m intervals (e.g., 2 = 2000 m deep). Bottom diagrams show topographic cross-sections along two latitudinal survey lines shown in the map, which are based on the results of seismic survey (Scientific Party on Board R/V *Kaiyo*, 1990). CB = central basin. ER = eastern ridge.

as young as <0.3 Ma. Older samples derived from cliffs along horsts, or from the Vot Tande area further south in the JCT. Such rocks are compositionally akin to the lavas of the modern central volcanic chain, and probably represent the pre-rifting basement of the arc. Therefore volcanic activity related to rifting probably occurred only in the northern half of the JCT, and since 2–3 Ma.

Description of samples

Northern part of the JCT (N-JCT)

Basalt and dacite were recovered from the N-JCT (see Appendix). The basalt is vesicular and aphyric, with microphenocrysts of plagioclase and rarely augite ± olivine, are set in an intersertal to intergranular groundmass with a diktytaxitic texture. Plagioclase is An_{90-70} , and olivine microphenocrysts are Fo_{88-77} . Augite has $Mg/(Mg + Fe^{2+})$ values (mg) of 0.90–0.88. Dacite and rare andesite are porphyritic (up to vol. 10%) with phenocrysts of plagioclase, augite, orthopyroxene and magnetite. They show fluidal textures, in which plagioclase and vesicles are elongated along flow planes. The groundmass is composed of glass and micro-lites. Plagioclase occurs as clear, slightly zoned (An_{70-44} in andesite, An_{46-23} in dacite) to about 2.5 mm long. Augite has mg of 0.73–0.64 in both andesite and dacite, while orthopyroxene has mg of 0.72–0.65 in andesite and of 0.71–0.58 in dacite.

Central part of the JCT (C-JCT)

Rocks recovered from the C-JCT are basaltic andesite and andesite. Altered gabbro and diorite were also sampled from the western margin of the C-JCT. Basaltic andesite is porphyritic, with phenocrysts of plagioclase, augite and olivine set in an intersertal groundmass. Plagioclase phenocrysts occur as skeletal crystals up to 1.5 mm long. Some samples contained glomerophyric aggregates composed of olivine, augite and plagioclase (up to 2 mm across). Andesites are porphyritic with 30–40 vol.% phenocrysts, including plagioclase, augite, orthopyroxene, hornblende and magnetite, set in an intersertal groundmass. Plagioclase phenocrysts are up to 2 mm long with complex zoning, and

many are corroded, with honeycomb textures. Hornblende phenocrysts to 1 mm long are rare, with green-brown to dark brown pleochroism and opacite rims. Glass-rich inclusions in the andesite to 5 mm across are sometimes present.

Southern part of the JCT (S-JCT)

Volcanic rocks were recovered from fault scarps developed along both sides of the ridges. Many are volcanoclastic or pumiceous (see Appendix). Fresh augite + olivine-phyric basalt and pyroxene andesite were also recovered, and a plagioclase-phyric basalt (DT8-1; K3981) has given a K–Ar age of 3.7 ± 0.2 Ma. These rocks are considered to be basement of the Vanuatu arc, since they are compositionally similar to volcanic rocks on the active central volcanic islands of the Vanuatu arc.

Analytical methods

Whole-rock chemical analyses of JCT rocks were carried out via XRF and ICP. The XRF analyses were performed at either La Trobe University (Australia) or Kyushu University, and the REE analyses were done using ICP at Ibaraki University. Details of analytical techniques are given in Price et al. (1990), Nakada and Kamata (1991) and Tagiri and Fujinawa (1988). Representative analyses are listed in Table 1, which includes 5 samples from Monjaret (1989; major and trace elements by atomic absorption at the *Université de Bretagne Occidentale*, and some trace elements by INAA at the *Laboratoire Pierre Süe*, Saclay). Several samples were analyzed in both laboratories to check analytical accuracy, and these show good agreement except for very low levels of Cr and Nb via XRF.

Geochemistry of the JCT volcanic rocks

According to Miyashiro's SiO_2 – FeO^* (total iron as FeO)/ MgO diagram, the JCT volcanic rocks cluster on the divide between the tholeiitic and calc-alkaline fields (Fig. 3). These rocks show SiO_2 bimodality, with a gap broadly between 55% and

TABLE 1a

Chemical compositions of representative volcanic rocks recovered from the northern part of the Jean Charcot Trough

No. Project Age ^c	D2M5 ^a SEAPSO	D2-1 ^b KAIYO	D5M5 ^a SEAPSO	D3M1 ^a SEAPSO 1.8	D1M8 ^a SEAPSO 1.1	D1M9 ^a SEAPSO 1.5	K3151 KAIYO	DT5-2 ^b KAIYO <0.3	K3154 KAIYO	DT5-5 ^b KAIYO
SiO ₂	49.00	49.28	49.50	57.90	65.20	64.00	66.43	66.77	66.96	66.09
TiO ₂	1.15	0.55	0.85	1.82	0.90	0.77	0.85	0.95	0.86	0.96
Al ₂ O ₃	16.50	18.01	16.65	15.75	16.20	15.50	15.33	15.38	15.52	15.28
Fe ₂ O ₃	1.52	9.02	1.52	1.39	0.75	0.78	1.40	5.23	1.20	5.26
FeO	7.76		7.76	7.11	3.84	4.00	3.00		3.22	
MnO	0.14	0.17	0.16	0.19	0.15	0.18	0.16	0.20	0.16	0.20
MgO	8.55	7.11	7.35	2.41	1.21	2.19	1.19	1.16	1.17	1.17
CaO	12.40	13.70	13.05	5.58	3.56	4.53	3.18	3.26	3.23	3.29
Na ₂ O	2.30	1.74	2.44	5.34	6.55	5.80	5.56	6.76	6.21	6.71
K ₂ O	0.28	0.28	0.31	0.71	0.88	0.71	0.85	0.92	0.86	0.91
P ₂ O ₅	0.05	0.10	0.05	0.18	0.15	0.15	0.24	0.20	0.25	0.22
H ₂ O ⁺	0.12		0.03	0.79	0.72	0.78	0.73		0.60	
H ₂ O ⁻	0.14		0.11	0.11	0.05	0.09	1.28		0.08	
Total	99.91	99.96	99.78	99.28	100.16	99.48	100.20	100.83	100.32	100.09
Rb	3	3	3	9	13	11	13.5	13	14.2	13
Sr	214	298	213	218	182	149	172	164	174	164
Ba	54	167	47	119	171	131	193	211	193	
V	216	240	196	73		70	22	29	20	24
Cr	260	61	159	5		25	2		2	
Ni	102	52	46	2		16	5		5	
Cu							2			
Zn							95		88	
Y		11					52	52	53	46
Zr	60	27	40	140	213	204	220	227	223	229
Nb		1					11	10	11	9
Ta	0.094		0.079	0.41	0.60	0.51				
Th	0.32		0.23	0.83	1.53	1.2	1.4			
Pb							3.1		3.3	
Ga							18		19	
La	3.4	3.0	2.5	9.2	13.7	11.7	13.0	15.4	13.0	14.8
Ce	7.0	6.8	7.0	25.9	28.0	30.1	35.0	36.3	32.0	33.9
Nd		5.2						22.8		21.7
Sm	2.3	2.0	1.8	5.6	6.1	5.7		7.6		7.2
Eu	0.93	0.71	0.72	2.1	1.9	2.0		2.2		2.0
Gd		2.0						7.9		7.2
Tb	0.46		0.39	1.2	1.2	1.2				
Dy		2.2						8.7		7.9
Er		1.4						5.9		5.2
Yb	2.0	1.3	1.90	4.7	6.2	5.2		6.1		5.3
Lu		0.19						0.89		0.80
Analy.	UBO/PS	KU/IU	UBO/PS	UBO/PS	UBO/PS	UBO/PS	LTU	KU/IU	LTU	KU/IU

^aData from Monjaret (1989). ^bTotal iron as Fe₂O₃. ^cK-Ar ages in Ma (Monjaret et al., 1991; S. Nakada, unpubl. data, 1990). UBO/PS=atomic absorption at *Université de Bretagne Occidentale* (analyst: J. Cotten), and INAA at Pierre Süe (J.L. Joron). KU/IU=XRF at Kyushu University (S. Nakada) and ICP at Ibaraki University (A. Fujinawa). LTU=XRF at La Trobe University (P. Maillet and I. Mac Cabe).

60% SiO₂. All the N-JCT lavas are depleted in K₂O (Fig. 3), and dacite is notably Na-rich, with up to 6% Na₂O (Table 1; Fig. 4). Rocks from the

C-JCT are slightly more K₂O-enriched than those from the N-JCT, but still have low K₂O contents, compared with rocks from the S-JCT and the

TABLE 1b

Chemical compositions of representative volcanic rocks recovered from the central part of the Jean Charcot Trough

No. Project Age ^c	K4150 KAIYO	K4151 KAIYO	D5-2 ^b KAIYO	K4153 KAIYO	K4155 KAIYO	D5-X ^b KAIYO <0.3	cy1-1 ^b SAVANES	cy3-1 ^b SAVANES	cy3-4 ^b SAVANES	cy3-6 ^b SAVANES
SiO ₂	59.07	59.15	58.48	59.12	59.10	58.48	61.55	53.66	53.71	54.79
TiO ₂	0.95	0.92	1.01	0.93	0.93	0.99	0.62	1.34	1.37	0.92
Al ₂ O ₃	17.57	17.59	17.54	17.68	17.54	17.60	17.60	16.18	17.76	17.79
Fe ₂ O ₃	2.55	2.50	7.29	2.55	2.57	7.22	5.26	8.91	9.23	9.00
FeO	3.95	3.93		3.89	3.88					
MnO	0.17	0.17	0.20	0.17	0.17	0.20	0.16	0.17	0.17	0.16
MgO	3.07	3.06	2.90	3.03	3.07	2.92	2.19	5.66	5.22	4.28
CaO	6.68	6.70	6.77	6.68	6.70	6.74	5.12	9.07	9.60	9.28
Na ₂ O	3.60	3.62	4.64	3.70	4.41	4.73	5.27	3.90	3.29	3.40
K ₂ O	0.94	0.92	0.97	0.93	0.94	0.98	1.06	0.72	0.70	0.65
P ₂ O ₅	0.26	0.26	0.23	0.26	0.26	0.24	0.21	0.22	0.15	0.14
H ₂ O ⁺	0.90	0.77		0.81	0.73					
H ₂ O ⁻	0.21	0.18		0.19	0.22					
Total	99.92	99.77	100.03	99.94	100.52	100.10	99.03	99.83	101.20	100.43
Rb	12.7	12.1	13	12.4	12.5	11				
Sr	286	288	273	288	287	265				
Ba	180	180	217	183	188	196				
V	140	133	176	135	135	189				
Cr	3	2	5	2	3	8				
Ni	6	6	9	6	7	7				
Cu	73	82		90	81					
Zn	78	70		78	80					
Y	31.7	31.5	29	31.7	31.5	30	22	38	24	17
Zr	154	154	167	155	155	163				
Nb	11	12	10	12	12	10				
Th		1.5			1.3					
Pb	3.2	3		3	3.4					
Ga	20	20		19	19					
La	12.0	11.0	12.6	13.0	13.0	12.2	13.3	8.4	4.9	5.3
Ce	27.0	28.0	28.7	24.0	27.0	27.2	27.1	22.4	11.9	11.9
Nd			15.8			15.5	14.6	16.5	9.4	8.6
Sm			4.8			4.9	4.0	6.2	3.5	3.0
Eu			1.5			1.5	1.2	1.8	1.2	1.0
Gd			4.6			4.6	3.6	6.2	4.0	3.0
Tb										
Dy			5.1			5.1	3.9	6.9	4.3	3.3
Er			3.4			3.2	2.5	4.2	2.7	2.1
Yb			3.5			3.3	2.7	4.1	2.6	1.9
Lu			0.51			0.51	0.42	0.60	0.38	0.30
Analy.	LTU	LTU	KU/IU	LTU	LTU	KU/IU	KU/IU	KU/IU	KU/IU	KU/IU

modern volcanic chain. Basalts are low-K tholeiites, and have compositional characteristics akin to MORB and BABB erupted at the main NFB spreading center (Eissen et al., 1991; Price and Kroenke, 1991). Incompatible element ratios (e.g. K/Rb, Ba/Rb, Zr/Rb, La/Rb, Ba/La, Nb/La and Ba/Zr in Fig. 5a and b) are almost identical in the

basaltic and evolved rocks of the N-JCT and C-JCT except one altered basalt sample (D2-1), but Y/Rb values are slightly but consistently higher in the N-JCT rocks (Fig. 5a). These same element ratios are almost identical to those in the NFB basalts, but quite unlike those from the active volcanic chain and S-JCT, reinforcing our inter-

TABLE 1c

Chemical compositions of representative volcanic rocks recovered from the southern part of the Jean Charcot Trough

No.	K3981	DT8-1 ^b	DT8-2 ^b	DT8-3 ^b	DT9-4 ^b	DT9-5 ^b
Project	KAIYO	KAIYO	KAIYO	KAIYO	KAIYO	KAIYO
Age ^c		3.7±0.2				
SiO ₂	51.92	52.09	52.62	56.97	54.57	56.87
TiO ₂	0.70	0.73	0.76	0.77	0.95	0.80
Al ₂ O ₃	19.53	20.03	16.01	17.92	15.15	15.71
Fe ₂ O ₃	3.68	7.76	11.67	7.87	9.85	9.77
FeO	3.78					
MnO	0.14	0.16	0.21	0.18	0.18	0.16
MgO	2.86	2.65	3.99	2.34	4.39	3.85
CaO	8.80	8.85	9.19	7.30	8.54	7.60
Na ₂ O	2.81	3.59	2.71	3.66	2.86	2.57
K ₂ O	2.32	2.43	1.30	1.81	1.75	2.31
P ₂ O ₅	0.51	0.49	0.22	0.24	0.87	0.33
H ₂ O ⁺	1.29					
H ₂ O ⁻	1.70					
Total	100.04	98.78	98.68	99.06	99.11	99.97
Rb	33.5	38	20	31	37	47
Sr	1020	999	357	376	395	395
Ba	311	313	515	270	270	326
V	269	252	428	276	298	354
Cr	9	19	38	8	89	27
Ni	12	17	22	7	26	29
Cu	270					
Zn	84					
Y	19.7	18	19	22	22	16
Zr	92	109	58	88	80	76
Nb	5	2	1	4	4	5
Th						
Pb	5.6					
Ga	17					
La	14.0	14.3	6.3	9.0	8.5	7.6
Ce	30.0	31.7	12.3	19.4	18.7	17.1
Nd		17.8	8.5	10.9	11.1	9.6
Sm		4.8	2.8	3.4	3.4	3.0
Eu		1.4	0.86	1.1	1.0	0.84
Gd		3.6	2.8	3.5	3.4	2.6
Tb						
Dy		3.2	3.2	3.6	3.2	2.8
Er		1.9	2.1	2.3	2.1	1.8
Yb		1.8	2.0	2.3	2.1	1.7
Lu		0.22	0.34	0.32	0.32	0.29
Analy.	LTU	KU/IU	KU/IU	KU/IU	KU/IU	KU/IU

pretation that the volcanics recovered in the S-JCT are not related to arc rifting, but are basement rocks of the Vanuatu arc.

Basalts of the N-JCT have almost flat chondrite-normalized REE patterns (Fig. 6), and patterns for an andesite and the dacites are parallel to those

of the basalts. Basaltic andesites and andesites from the C-JCT show two styles of REE patterns, flat, and significantly LREE-enriched (Fig. 6). Rocks from the S-JCT show REE patterns similar to the latter. Lavas from the central volcanic chain also show two patterns, flat, and strongly

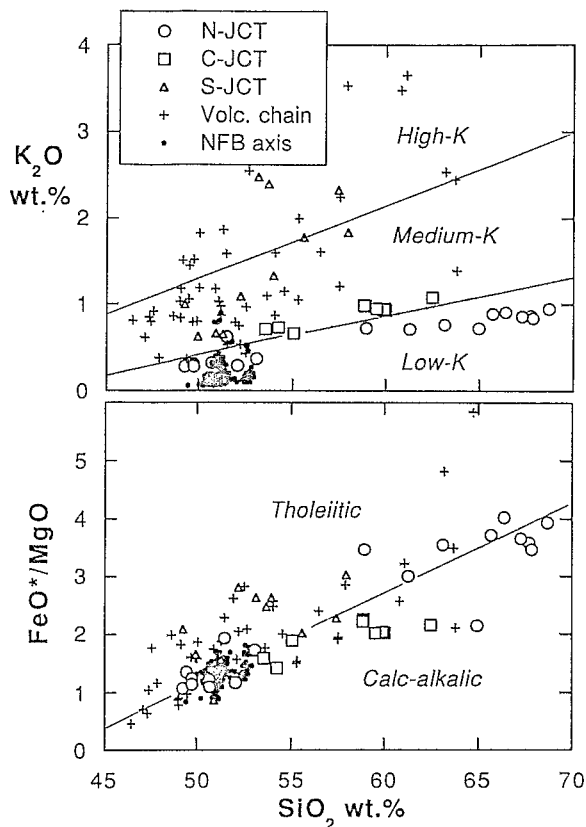


Fig. 3. SiO_2 - K_2O , and $-\text{FeO}^*/\text{MgO}$ plots for volcanic rocks from the Jean Charcot Trough, Vanuatu volcanic chain, and central spreading axis of North Fiji Basin. The sum of 10 major elements was recalculated to 100%, assuming total iron as FeO (FeO^*). Boundaries of low-, medium-, and high-K are from Ewart (1982), and between tholeiitic and calc-alkalic rocks from Miyashiro (1974). Analyses for the Vanuatu arc volcanic rocks are from Gorton (1977) and Barsdell et al. (1982), and for basalts in the central spreading axis of the North Fiji Basin from Eissen et al. (1991).

LREE-enriched. The flat patterns are for low-K basalts from Merelava Island (Barsdell et al., 1982) which sits on the western rim of the S-JCT. The other Vanuatu arc volcanoes in this northern section of the arc all show strongly LREE-enriched patterns. REE patterns for NFB are mostly LREE-depleted for the N-MORB-like basalts or flat for the BABB, and partly significantly LREE-enriched for the T-MORB (Eissen et al., 1993). HREE-levels are higher in the NFB basalts ($\times 10$ – 15 chondrite) than in the N-JCT basalts ($\times 5$ – 10).

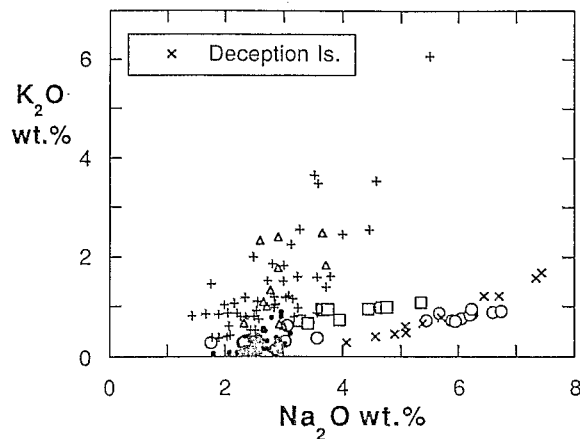
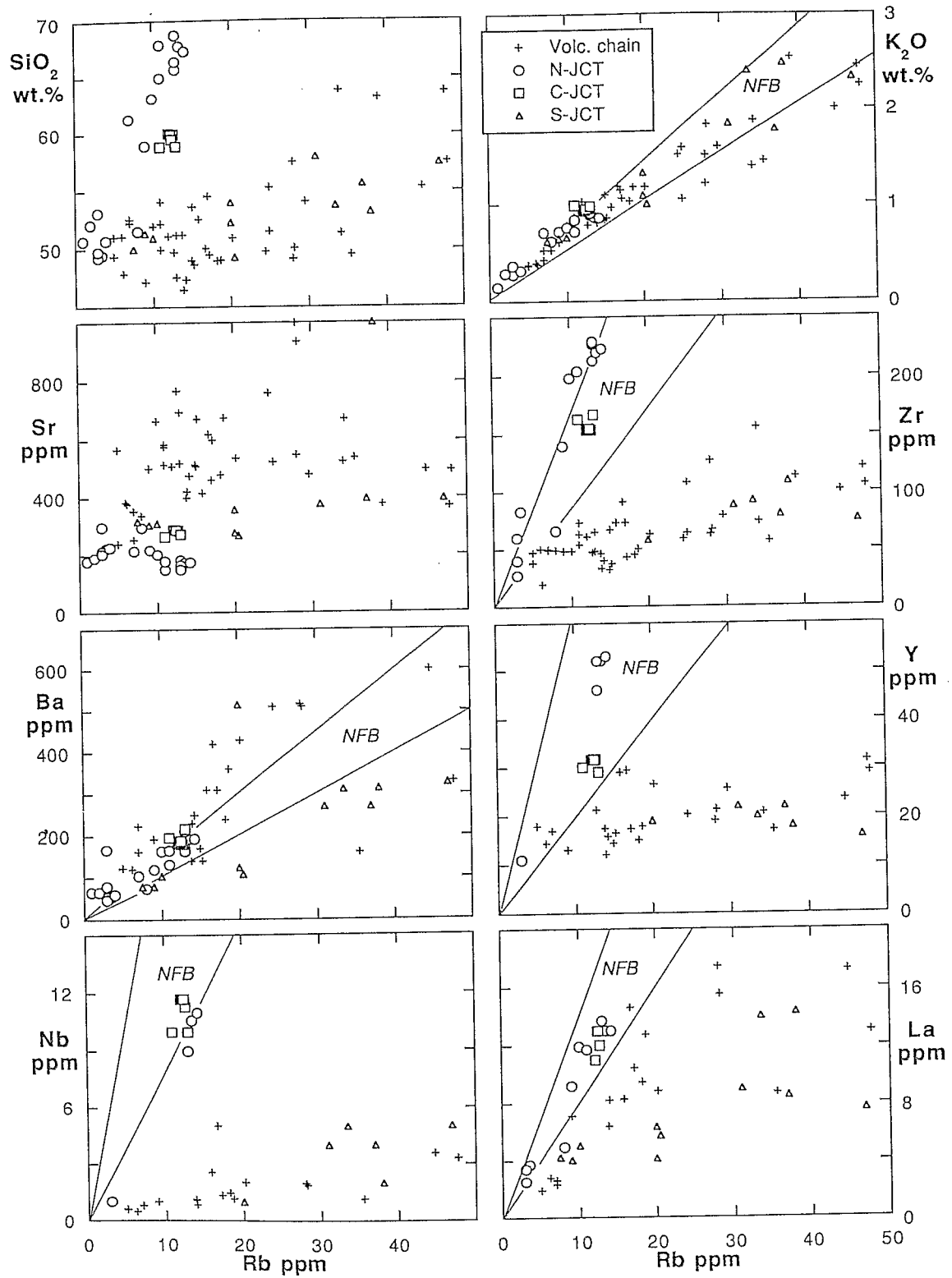


Fig. 4. Na_2O - K_2O plot for volcanic rocks from the Jean Charcot Trough, Vanuatu volcanic chain, and central spreading axis of North Fiji Basin. Analyses of volcanic rocks from Deception Island (Weaver et al., 1979) are shown for comparison. For symbols, see Fig. 3.

High-Na dacite

The high-Na characteristic of these N-JCT dacites is clearly not due to accumulation of plagioclase (An_{46-23}) phenocrysts, which themselves have $< 7\%$ Na_2O , as indicated by the relatively low Sr (< 200 ppm) and Al_2O_3 (17%) contents in the dacites. Almost identical incompatible element ratios between the low-K basalts and high-Na dacites suggest that some intimate petrogenetic relationship links these magma types.

Also shown on Fig. 3 together with lavas from the Vanuatu arc and JCT are some lavas from Deception Island in Bransfield Strait, the back-arc trough of the South Shetland arc that started opening around 1.5 Ma (Weaver et al., 1979). The high-Na dacites compositionally resemble trondhjemite or oceanic plagiogranite (Barker, 1979). Incompatible element patterns of high-Na dacites from the JCT and Deception Island normalized to oceanic plagiogranite of Pearce et al. (1984) are given in Fig. 7. Except for slight enrichment in large ion lithophile elements (LILE), both high-Na dacites are close to the reference plagiogranite. As the latter magma type is interpreted to have evolved via simple fractional crystallization of N-MORB (Pearce et al., 1984), our data suggest that extensive fractionation of a slightly LILE-enriched BABB or transitional-



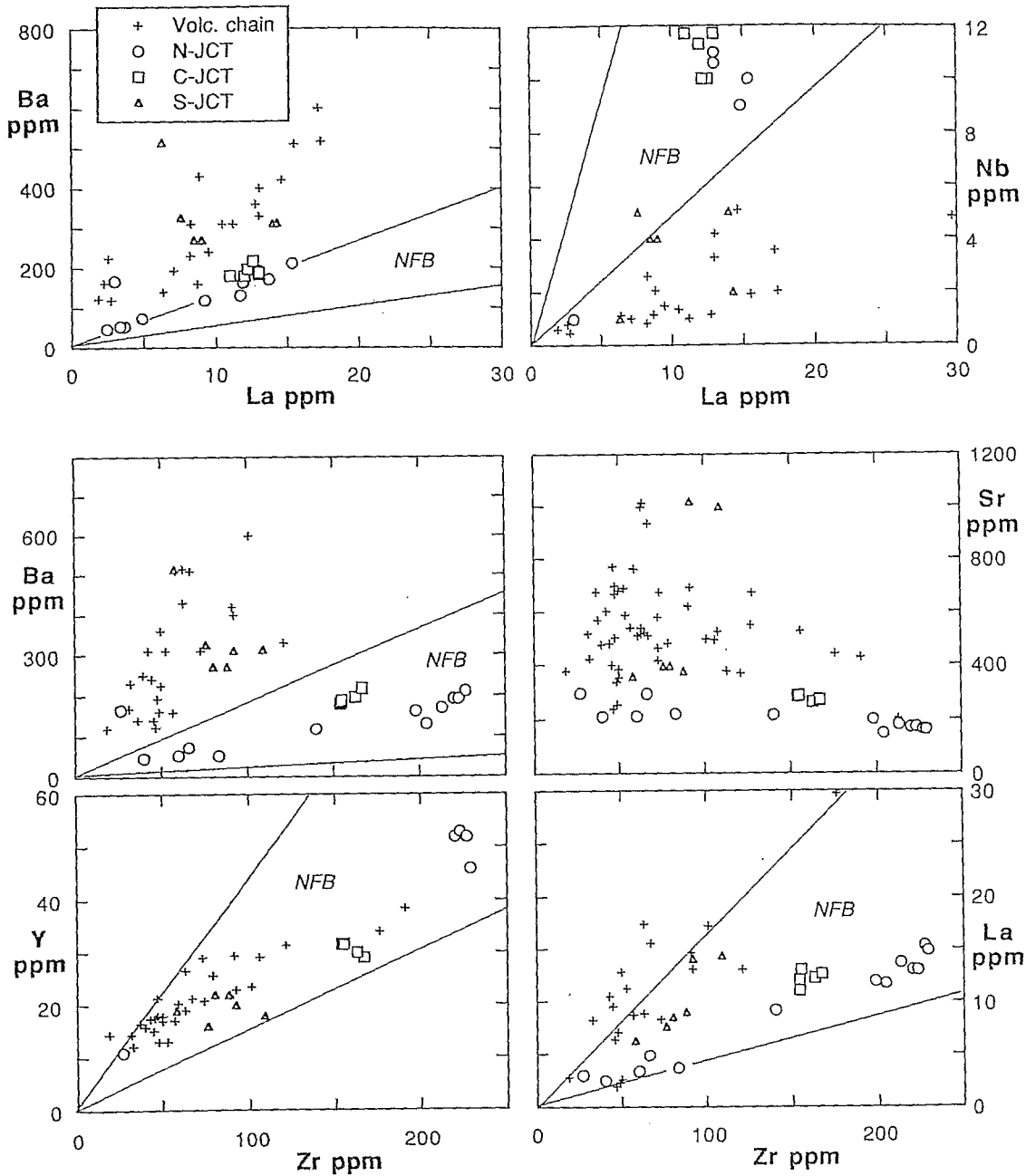


Fig. 5. Rb, La, and Zr variation diagrams for volcanic rocks from the Jean Charcot Trough. Analyses for rocks from the Vanuatu volcanic arc are from Gorton (1977) and Barsdell et al. (1982). The two straight lines sandwiching the NFB represent maximum and minimum values of elemental ratios for basalts from the central spreading axis of the North Fiji Basin (Eissen et al., 1991, 1993; Price and Kroenke, 1991).

MORB can generate the high-Na dacites. The high-Na dacite from Deception Island is more enriched in Zr and Th than the JCT dacite (Fig. 7). This probably reflects the source mantle's

enrichment in these elements beneath the Deception Island region, as the associated basalts are also more enriched in both elements (Weaver et al., 1979).

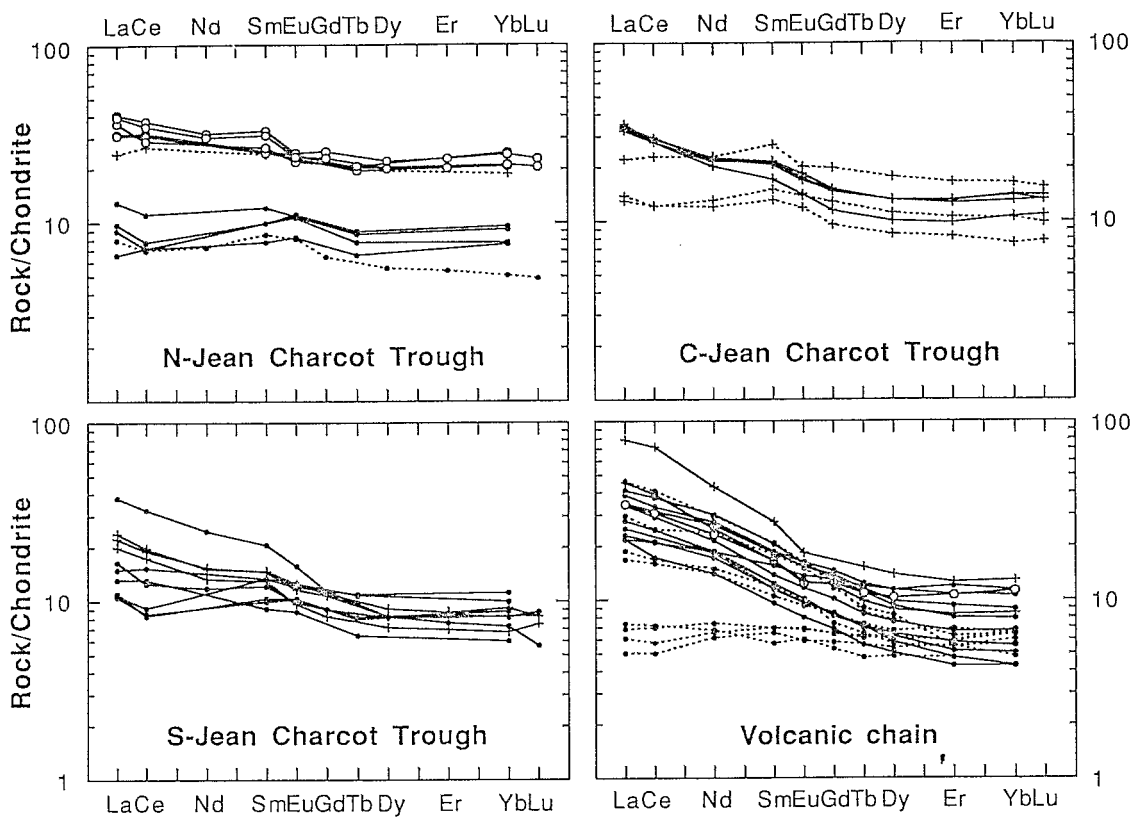


Fig. 6. Chondrite-normalized REE patterns for volcanic rocks from the Jean Charcot Trough and Vanuatu volcanic chain. \odot = basalt, $+$ = andesite, and \square = dacite. Data for Vanuatu chain are from Gorton (1977) and Barsdell et al. (1982). Chondrite values from Masuda (1975).

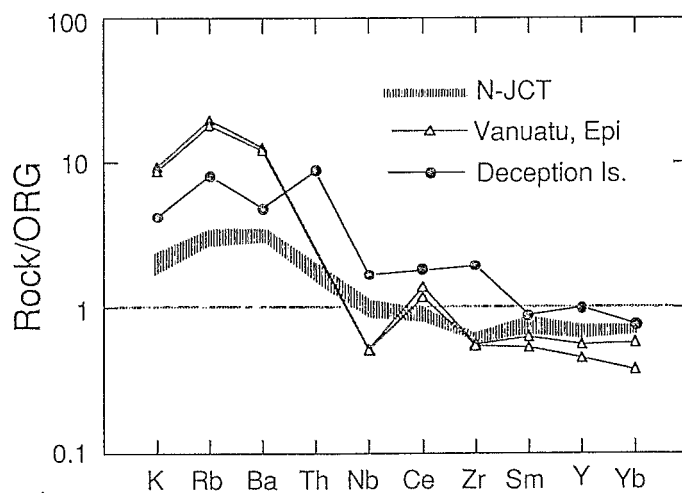


Fig. 7. Geochemical patterns of the high-Na dacites from the Jean Charcot Trough. Normalizing values of ocean ridge granite (ORG) is from Pearce et al. (1984). Dacites from Epi Volcano (Crawford et al., 1988) and Deception Island (Weaver et al., 1979) are shown for comparison.

Discussion

SiO₂ bimodality and partial melting

The SiO₂ bimodality noted for the N-JCT lavas might be explained by partial melting of crustal material by basaltic magmas. However, such an origin would seem to be precluded by the strong trace element similarities between the JCT basalts and dacites, and the fact that the basement of the JCT was almost certainly arc basalts and their cumulate complement. Partial melting of such rocks could not produce the geochemical coherence observed between the basalts and the high-Na dacites.

Partial melting of gabbros identical to the N-JCT low-K basalts could produce the high-Na dacites. Garnet and amphibole appear in constituents of gabbros at high pressure (> 10 kbar) and in hydrous condition, respectively (e.g., Green, 1982). These two minerals can not be accepted during partial melting in order to explain the chemical coherence between the basalts and dacites, because their participating creates different geochemical patterns (e.g., K/Rb and REE patterns). Thus, nearly dry conditions at relatively low pressure may be necessary for the partial melting hypothesis. However, melting experiments using MORBs (e.g., Grove et al., 1990) showed that partial melts in dry conditions at pressures less than 10 kbar are basaltic and basaltic andesite in composition, regardless of degrees of melting and pressures; 48 and 45% SiO₂, about 30% of melting at 1 atm and 8 kbar, respectively (Grove et al., 1990). Incompatible element relationship between the low-K basalts and high-Na dacites (see K and Ba in Table 1) requests a degree of melting of about 25%. Therefore, it is also unlikely to produce the high-Na dacites from the low-K gabbro via partial melting.

Fractionation of low-K basalt

Crawford et al. (1988) noted that dacite only occurs in volcanoes with large calderas in the Vanuatu arc, and suggested that the dacites are linked to associated basalts by fractional crystallization. They argued that the dacitic magmas repre-

sent differentiated liquid produced in large subvolcanic magma chambers by boundary-layer convection resulting from side-wall crystallization (e.g., McBirney et al., 1985): stagnant, highly differentiated liquids pool under the roof and on the nearly unmodified basaltic core of the magma chamber. The same model may explain the petrogenesis of the high-Na dacites from the N-JCT.

The Na₂O contents of the basaltic rocks of the JCT are not high compared with those from the NFB and other MORB (Fig. 4). This implies that the distinctive high-Na characteristics of the JCT dacite must be acquired during the differentiation process of the basaltic magma. As plagioclase is the dominant phenocryst in the basalt, two models could explain the high-Na contents: (1) fractionation of extremely calcic plagioclase, or (2) plagioclase is a subordinate phase in the fractionating assemblage. The JCT basalt plagioclase phenocrysts (An₇₀₋₉₀) are no more calcic than those in the adjacent and other arc volcanoes, but the arc dacites are never as Na-rich as those in the N-JCT (Ewart, 1982). A low proportion of plagioclase in a fractionation assemblage from a basaltic magma could be caused by either a high magma water content, or high-pressure crystallization. Plagioclase does not crystallize above 8 kbar (Green, 1982), and disappears at lower pressures if the magma contains a significant quantity of water. The low K₂O contents and lack of amphibole phenocrysts in the basalts and particularly in the high-Na dacites, do not support high water contents in the parental magma. It is considered unlikely that the distinctive high-Na feature of the N-JCT dacites is due to relatively high water contents of the parental basaltic magma.

Mass balance calculations (MacGPP program) using major elements (Table 2) and compositions of representative phenocrysts in the basalts and andesites (Monjaret, 1989) show that around 80% fractionation of the low-K basalt (D2M5) can produce the high-Na dacite (D1M8) via high-Na andesite (D3M1). The weight ratio of fractionating plagioclase to mafic minerals is close to 1:1. Rayleigh fractionation trace element testing of this model yields good fits for most trace elements, supporting the interpretation that the high-Na dacites can be derived from the low-K basalts via

TABLE 2

Mass-balance calculations testing derivation of high-Na dacite from basalt through andesite

	% Amount	SiO ₂	TiO ₂	Al ₂ O ₃	FeO*	MnO	MgO	CaO	Na ₂ O	K ₂ O	P ₂ O ₅
<i>Model A (Basalt-Andesite)</i>											
Parent D ₂ M ₅	1.000	49.25	1.16	16.58	9.17	0.14	8.59	12.46	2.31	0.28	0.05
Plag (An ₈₀)	0.348	47.85	0.00	33.59	0.00	0.00	0.00	16.29	2.20	0.07	0.00
Augite	0.263	52.55	0.30	2.24	7.79	0.05	16.91	20.05	0.12	0.00	0.00
Olivine	0.084	39.32	0.00	0.12	19.27	0.30	40.69	0.25	0.05	0.00	0.00
Magnetite	0.041	0.00	14.81	2.25	79.95	1.03	1.96	0.00	0.00	0.00	0.00
Daughter D ₃ M ₁	0.264	58.94	1.85	16.03	8.51	0.19	2.45	5.68	5.44	0.72	0.18
Daughter (calculated)		58.53	1.78	15.94	8.47	0.23	2.47	5.72	5.70	0.97	0.19
Differences		0.41	0.07	0.09	0.04	-0.04	-0.02	-0.04	-0.26	-0.25	-0.01
Sum of squares of residuals=		0.312									
<i>Model B (Andesite-Dacite)</i>											
Parent D ₃ M ₁	1.000	58.94	1.85	16.03	8.51	0.19	2.45	5.68	5.44	0.72	0.18
Plag (An ₆₁)	0.164	55.98	0.07	27.06	0.67	0.01	0.04	10.51	5.63	0.03	0.00
Orthopyroxene	0.014	52.93	0.34	0.92	20.15	0.98	23.19	1.49	0.00	0.00	0.00
Augite	0.078	50.45	0.83	2.78	12.04	0.54	14.01	18.93	0.39	0.03	0.00
Magnetite	0.055	0.00	18.23	2.75	75.25	0.62	3.06	0.10	0.00	0.00	0.00
Daughter D ₁ M ₈	0.690	65.65	0.91	16.31	4.55	0.15	1.22	3.58	6.60	0.89	0.15
Daughter (calculate)		65.37	1.13	16.26	4.47	0.15	1.26	3.56	6.50	1.04	0.27
Differences		0.28	-0.22	0.05	0.08	0.00	-0.04	0.02	0.10	-0.15	-0.12
Sum of squares of residuals=		0.185									

MacGPP, a program package for creating and using geochemical data files, produced by D.J. Geist, A.R. McBirney and B.H. Baker in 1989 was used. All analytical data were recalculated to 100% without water.

crystal fractionation (Table 3). A similar possibility was proposed by Weaver et al. (1979) for the Deception high-Na dacites, and may be reinforced by identical Sr isotope ratios for the Deception basalts and high-Na dacites.

Source material of the JCT lavas

As the JCT has developed within an oceanic arc, the mantle beneath the JCT at the time it commenced rifting was presumably typical of sub-arc upper mantle. However, the strong compositional similarity between the NFB spreading center basalts and the JCT basalts implies that their source mantle compositions were also very similar. Replacement of sub-arc mantle by N-MORB mantle has occurred during rifting of the JCT. Deep earthquakes indicate that presence of a subducted slab beneath the JCT, implying that diapiric ascent of N-MORB mantle to initiate JCT spreading would have to pierce this slab, an

unlikely scenario. An alternative model involves westward injection about 2–3 Ma of N-MORB source mantle that was originally located beneath the NFB. Tatsumi et al. (1989) also proposed that asthenospheric injection into the mantle wedge of NE Japan initiated opening of the Sea of Japan. Partial melting of the invading N-MORB mantle produced parental basalts for the JCT, which were trapped at relatively deep levels in the arc crust (compared to MORB magma chambers at steady-state ridges) and fractionated to produce the high-Na dacites.

Compared to most of NFB basalts, low-K basalts of the N-JCT are relatively enriched in K₂O/SiO₂ (Figs. 3 and 4), but have lower HREE levels. This may reflect smaller degrees of melting of a source material that is more refractory (residual) than the primary N-MORB source of the NFB basalts. Furthermore, volcanic rocks are more enriched in K₂O/SiO₂ and lower in Y/Rb in the C-JCT than the N-JCT (Figs. 3–5), implying

TABLE 3

Trace element abundances predicted for andesite and dacite magmas derived from basalt through Rayleigh fractionation. Models A and B are equivalent to those in Table 2

	Basalt	Andesite		Dacite		Partition coefficients*				
	D2M5	D3M1	Model A (calc.)	D1M8	Model B (calc.)	plag	ol	cpx	opx	mgt
Sr	214	218	221	182	211	2.0	0	0	0	0
Rb	3	9	11	13	13	0	0	0	0	0
Ba	54	119	162	171	161	0	0	0	0	0
La	3.4	9.2	9.0	13.7	12.0	0.3	0	0.3	0	0.3
Ce	7.0	25.9	19.0	28.0	34.3	0.2	0	0.4	0	0.2
Sm	2.3	5.6	6.7	6.1	7.6	0.1	0	0.4	0.4	0.1
Eu	0.9	2.1	1.4	1.9	2.4	0.7	0.03	1.0	0.3	0
Yb	2.0	4.7	4.5	6.2	6.1	0.1	0.03	0.9	0.5	0
K ₂ O%	0.28	0.71	0.85	0.88	0.97	0.2	0	0.2	0	0

*Sources of partition coefficients are Gill (1981) and Wilson (1989).

smaller degrees of melting of a source mantle just beneath the C-JCT.

Conclusions

The Jean Charcot Trough has developed within the intra-oceanic Vanuatu island arc since 2–3 Ma. Active tectonic and magmatic activity is now restricted to the northern half of the trough, where volcanic cones composed of andesite and basalt have been recognized, although dominant magmatism shows SiO₂ bimodality, with low-K basalt and comagmatic high-Na, low-K dacite. The low-K basalt is compositionally akin to N-MORB and BABB from the North Fiji Basin. The high-Na dacite is shown to have evolved from this basalt by around 80% simple fractional crystallization at relatively high pressure. This fractionation may have occurred during side-wall crystallization in a deep-crust magma chamber. Westward injection of dioritic source mantle similar to that of the

North Fiji Basin basalts may have caused rifting of the JCT.

Acknowledgements

The STARMER project is funded by the Science and Technology Agency (STA) of Japan and the *Institut Français de Recherche pour l'Exploitation de la Mer* (IFREMER), and cooperated with the South Pacific Applied Geoscience Commission (SOPAC). Research was done using R/V *Kaiyo* of the Japan Marine Science and Technology Center (JAMSTEC) in 1989 (KAIYO 89) and the *Cyana* a submersible on R/V *Le Noroit* of IFREMER in 1991–1992 (SAVANES 91–92). We thank the scientific parties of KAIYO 89 and SAVANES 91–92, especially J.P. Eissen, E. Ruellan, M. Tanahashi and R.C. Price for their coordination, T. Fujii for his discussion, and A.J. Crawford and Eissen for their kind and careful reviews. We also thank captains and crews of both research vessels, and the *Cyana* team who made a wonderful sea-floor survey during the SAVANES cruise.

Appendix

Localities of samples recovered from Jean Charcot Trough during STARMER cruises

Sample no.	Cruise	St. no.	Latitude	Longitude	Depth (m)	Remarks on collected samples
Northern Part (N-JCT)						
D2-1	K	33	12°10.3'S– 12°10.3'S	167°47.0'E– 167°46.3'E	2038–1658	Slightly altered, highly vesiculated basalt.
K3151, K3154, DT5-2, -5	K	31	12°11.6'S– 12°11.6'S	167°34.9'E– 167°35.4'E	915–459	Fresh lava blocks of glassy, moderately vesiculated dacite. Close to point D1 of SEAPSO 2.
DT6	K	31	12°12.5'S– 12°12.5'S	167°37.6'E– 167°39.3'E	1242–1618	Pumice and lava fragments of aphyric, glassy basaltic andesite and andesite.
Central Part (C-JCT)						
K4150, K4151, K4153, K4155, D5-2, D5-X	K	41	12°33.3'S– 12°33.2'S	167°40.6'E– 167°40.8'E	1425–1284	Fresh massive blocks of andesite lavas collected near the summit of volcano.
cy1-41-R1	S	41	12°32.0'S	167°40.4'E	1905	Fresh gray-colored andesite.
cy1-41-R2	S	41	12°32.8'S	167°40.8'E	1486	Fresh, glassy, plagioclase-phyric andesite.
cy2-41-R1	S	41	12°32.2'S	167°42.8'E	2134	Strongly silicified volcanic rock.
cy2-41-R2	S	41	12°33.2'S	167°41.7'E	1176	Altered andesite.
cy3-41-R1	S	41	12°31.7'S	167°45.1'E	2412	Pillow lava; fresh porous basaltic andesite.
cy3-41-R2	S	41	12°31.4'S	167°45.2'E	2365	Pillow lava, fresh aphyric basaltic andesite.
cy3-41-R4	S	41	12°31.5'S	167°45.2'E	2203	Pillow lava, fresh aphyric basaltic andesite.
cy3-41-R5	S	41	12°32.0'S	167°45.8'E	2018	Pillow lava, slightly altered basaltic andesite.
cy3-41-R6	S	41	12°32.4'S	167°47.2'E	1550	Pillow lava, fresh aphyric basaltic andesite.
cy5-41-R1	S	41	12°39.6'S	167°33.8'E	2183	Medium-grained pyroxene gabbro.
cy5-41-R4	S	41	12°38.9'S	167°33.1'E	1668	Moderately altered pyroxene diorite.
Southern Part (S-JCT)						
DT7	K	39	12°51.5'S– 12°51.5'S	167°49.9'E– 167°47.5'E	3077–1540	Tuff and pumice.
K3981, DT8-1, DT8-2, DT8-3	K	39	12°51.5'S– 12°52.2'S	167°50.5'E– 167°51.0'E	2984–2130	Tuff and lava blocks of andesite and basalt. DT8-1 is fresh plag-phyric ol-aug basalt.
DT9-4, DT9-5	K	42	13°19.9'S– 13°19.9'S	167°55.8'E– 167°56.5'E	2140–1650	Tuff, pumice, and lava blocks of vesiculated, porphyritic andesite.

Cruise name: K = KAIYO 89, S = SAVANES 91–92. Samples were taken using deep tow and chain bag during KAIYO 89, and *Cyana* submersible during SAVANES 91–92.

References

- Barker, F., 1979. Trondhjemite: Differentiation, environment and hypotheses of origin. In: F. Barker (Editor), *Trondhjemites, Dacites, and Related Rocks*. (Developments in Petrology, 6.) Elsevier, Amsterdam, pp. 1–12.
- Barsdell, M., Smith, I.E.M. and Sporli, K.B., 1982. The origin of reversed geochemical zoning in the northern New Hebrides volcanic arc. *Contrib. Mineral. Petrol.*, 81: 148–155.
- Charvis, P. and Pelletier, B., 1989. The northern New Hebrides back-arc troughs: history and relation with the North Fiji basin. *Tectonophysics*, 170: 259–277.
- Collot, J.Y. and Fisher, M.A., 1991. The collision zone between the north d'Entrecasteaux Ridge and the New Hebrides island arc. 1. Sea Beam morphology and shallow structure. *J. Geophys. Res.*, 96: 4451–4478.
- Crawford, A.J., Greene, H.G. and Exon, N.F., 1988. Geology, petrology and geochemistry of submarine volcanoes around Epi island, New Hebrides island arc. In: H.G. Greene and F.L. Wong (Editors), *Geology and Offshore Resources of Pacific Island Arcs—Vanuatu Region*. Circum-Pacific Council. Energy Mineral Resour. Earth Sci. Ser., 8: 301–327.
- Dupuy, C., Dostal, J., Marcelot, G., Bougault, H., Joron, J.L. and Treuil, M., 1982. Geochemistry of basalts from central and southern New Hebrides arc: Implication for their source rock composition. *Earth Planet. Sci. Lett.*, 60: 207–225.

- Eggins, S.M., 1993. Origin and differentiation of picritic arc magmas, Ambae (Aoba), Vanuatu. *Contrib. Mineral. Petrol.*, 114: 79–100.
- Eissen, J.P., Lefevre, C., Maillet, P., Morvan, G. and Nohara, M., 1991. Petrology and geochemistry of the central North Fiji Basin spreading center (Southwest Pacific) between 16°S and 22°S. In: K.A.W. Crook (Editor), *The Geology, Geophysics and Mineral Resources of the South Pacific*. *Mar. Geol.*, 98: 201–239.
- Eissen, J.P., Nohara, M. and Cotten, J., 1993. The North Fiji Basin basalts and their magma sources: part I. Trace and rare earth elements constraints. In: J.-M. Auzende and T. Urabe (Editors), *North Fiji Basin: STARMER French–Japanese Program*. *Mar. Geol.*, 116: 153–178.
- Ewart, A., 1982. The mineralogy and petrology of Tertiary–Recent orogenic volcanic rocks: with special reference to the andesitic–basaltic compositional range. In: R.S. Thorpe (Editor), *Andesites. Orogenic Andesites and Related Rocks*. Wiley, New York, pp. 25–95.
- Gill, J.B., 1981. *Orogenic Andesites and Plate Tectonics*. Springer, New York, 390 pp.
- Gorton, M.P., 1977. The geochemistry and origin of quaternary volcanism in the New Hebrides. *Geochim. Cosmochim. Acta*, 41: 1257–1270.
- Green, T.H., 1982. Anatexis of mafic crust and high pressure crystallization of andesite. In: R.S. Thorpe (Editor), *Andesites. Orogenic Andesites and Related Rocks*. Wiley, New York, pp. 465–487.
- Grove, T.L., Kinzler, R.J. and Bryan, W.B., 1990. Natural and experimental phase relations of lavas from Serocki Volcano. *Proc. ODP, Sci. Results*, 106/109: 9–17.
- Louat, R. and Pelletier, B., 1989. Seismotectonics and present-day relative motions in the New-Hebrides–North Fiji Basin region. *Tectonophysics*, 167: 41–55.
- Louat, R., Hamburger, M. and Monzier, M., 1988. Shallow and intermediate-depth seismicity in the New Hebrides arc: constraints on the subduction process. In: H.G. Greene and F.L. Wong (Editors), *Geology and Offshore Resources of Pacific Island Arcs—Vanuatu Region*. Circum-Pacific Council. *Energy Mineral Resour. Earth Sci. Ser.*, 8: 329–356.
- Macfarlane, A., Carney, J.N., Crawford, A.J. and Greene, H.G., 1988. Vanuatu—a review of the onshore geology. In: H.G. Greene and F.L. Wong (Editors), *Geology and Offshore Resources of Pacific Island Arcs—Vanuatu Region*. Circum-Pacific Council. *Energy Mineral Resour. Earth Sci. Ser.*, 8: 45–91.
- Maillet, P., Monzier, M. and Lefèvre, C., 1986. Petrology of Matthew and Hunter volcanoes, south New Hebrides island arc (southwest Pacific). *J. Volcanol. Geotherm. Res.*, 30: 1–27.
- Masuda, A., 1975. Abundances of monoisotopic REE consistent with Leedy chondrite values. *Geochem. J.*, 9: 183–184.
- McBirney, A.R., Barker, B.H. and Nilson, R.H., 1985. Liquid fractionation, Part I: Basic principles and experimental simulations. *J. Volcanol. Geotherm. Res.*, 24: 1–24.
- Miyashiro, A., 1974. Volcanic rocks series in island arcs and active continental margins. *Am. J. Sci.*, 274: 321–355.
- Monjaret, M.C., 1989. Le magmatisme des fossés à l'arrière de l'arc des Nouvelles Hébrides (Vanuatu) (Campagne SEAPSO 2 du N/O Jean Charcot)—Chronologie, pétrologie et géochimie. Implications géodynamiques. Thesis Univ. Bretagne Occidentale, Brest, 490 pp.
- Monjaret, M.C., Bellon, H. and Maillet, P., 1991. Magmatism of the troughs behind the New Hebrides island arc (RV Jean Charcot SEAPSO 2 cruise): K–Ar geochronology and petrology. *J. Volcanol. Geotherm. Res.*, 46: 265–280.
- Monzier, M., Danyushevsky, L.V., Crawford, A.J., Bellon, H. and Cotten, J., 1993. High-Mg andesites from the southern termination of the New Hebrides island arc (SW Pacific). *J. Volcanol. Geotherm. Res.*, 57: 193–217.
- Nakada, S. and Kamata, H., 1991. Temporal change in chemistry of magma source under central Kyushu, southwest Japan: Progressive contamination of mantle wedge. *Bull. Volcanol.*, 53: 182–194.
- Pearce, J.A., Harris, N.B.W. and Tindle, A.G., 1984. Trace element discrimination diagrams for the tectonic interpretation of granitic rocks. *J. Petrol.*, 25: 956–983.
- Picard, C., Monzier, M., Eissen, J.P. and Robin, C., 1993. Concomitant evolution of the tectonic environment and geochemistry of the MK to HK volcanic sequences at Ambrym Volcano (Vanuatu–New Hebrides Arc). *J. Geol. Soc. London*, in press.
- Price, R.C., Johnson, L.E. and Crawford, A.J., 1990. Basalt of the North Fiji Basin: the generation of back-arc basin magmas by mixing of depleted and enriched mantle sources. *Contrib. Mineral. Petrol.*, 105: 106–121.
- Price, R.C. and Kroenke, L.W., 1991. Tectonics and magma genesis in the northern North Fiji Basin. In: K.A.W. Crook (Editor), *The Geology, Geophysics and Mineral Resources of the South Pacific*. *Mar. Geol.*, 98: 241–258.
- Récy, J., Pelletier, B., Charvis, P., Genard, M., Monjaret, M.C. and Maillet, P., 1990. Structure, âge et origine des fossés arrière-arc des Nouvelles-Hébrides (Sud-Ouest Pacifique). *Oceanol. Acta*, 10: 165–182.
- Roca, J.L., 1978. Essai de détermination du champ de contraintes dans l'archipel des Nouvelles-Hébrides. *Bull. Soc. Géol. Fr.*, 20: 511–519.
- Scientific Party on Board R/V Kaiyo, 1990. KAIYO 89 cruise in the northern Fiji Basin and Vanuatu back-arc troughs. *STARMER Cruise Rep.*, 5, 152 pp.
- Scientific Party on Board R/V Le Noroit, 1992. SAVANES 91–92 cruise with Cyana submersible in the northern Vanuatu back-arc troughs. *STARMER Cruise Rep.*, 8, 51 pp.
- Tagiri, M. and Fujinawa, A., 1988. Chemical analysis of REE and trace metals in GSJ rock reference samples by ICP. *Jpn. Assoc. Mineral. Petrol. Econ. Geol.*, 81: 102–106.
- Tatsumi, Y., Otofujii, Y., Matsuda, T. and Nohda, S., 1989. Opening of the Sea of Japan back-arc basin by asthenospheric injection. *Tectonophysics*, 166: 317–329.
- Weaver, S.D., Saunders, A.D., Pankhurst, R.J. and Tarney, J., 1979. A geochemical study of magmatism associated with the initial stages of back-arc spreading. *Contrib. Mineral. Petrol.*, 68: 151–168.
- Wilson, M., 1989. *Igneous petrogenesis: A global tectonic approach*. Unwin Hyman, London, 466 pp.

**Special Issue: North Fiji Basin: STARMER French-Japanese Program**
Edited by J.-M. Auzende and T. Urabe

Introduction	1
800-km-long N-S spreading system of the North Fiji Basin M. Tanahashi, K. Kisimoto, M. Joshima, P. Jarvis, Y. Iwabuchi, E. Ruellan and J.-M. Auzende	5
A possible triple junction at 14°50'S on the North Fiji Basin Ridge (Southwest Pacific)? J.-M. Auzende, E. Gràcia-Mont, V. Bendel, P. Huchon, Y. Lafoy, Y. Lagabrielle, G. de Alteriis and M. Tanahashi ..	25
Propagating rift and overlapping spreading center in the North Fiji Basin E. Ruellan, P. Huchon, J.-M. Auzende and E. Gràcia	37
The western Fiji Transform Fault and its role in the dismemberment of the Fiji Platform P. Jarvis, J. Hughes-Clarke, D. Tiffin, M. Tanahashi and L. Kroenke	57
Kinematics of active spreading in the central North Fiji Basin (Southwest Pacific) P. Huchon, E. Gràcia, E. Ruellan, M. Joshima and J.-M. Auzende	69
Magnetic anomaly patterns around the central rift area in the North Fiji Basin: Inversion approach for detailed structure M. Joshima, Y. Iwabuchi and S. Ookuma	89
Crustal structure variation along the central rift/ridge axis in the North Fiji Basin: Implications from seismic reflection and refraction data K. Kisimoto, M. Tanahashi and J.-M. Auzende	101
Geology and geochemistry of a 800 m section through young upper oceanic crust in the North Fiji Basin (Southwest Pacific) Y. Lagabrielle, J.-M. Auzende, J.-P. Eissen, M.-C. Janin and J. Cotten	113
Multi-scale morphologic variability of the North Fiji Basin ridge (Southwest Pacific) E. Gràcia, H. Ondréas, V. Bendel and STARMER Group	133
North Fiji Basin basalts and their magma sources: Part I. Incompatible element constraints J.-P. Eissen, M. Nohara, J. Cotten and K. Hirose	153
The North Fiji Basin basalts and their magma sources: Part II. Sr-Nd isotopic and trace element constraints M. Nohara, K. Hirose, J.-P. Eissen, T. Urabe and M. Joshima	179
High-Na dacite from the Jean Charcot Trough (Vanuatu), Southwest Pacific S. Nakada, P. Maillet, M.-C. Monjaret, A. Fujinawa and T. Urabe	197
Fluctuation of chemical compositions of the phase-separated hydrothermal fluid from the North Fiji Basin Ridge J.-i. Ishibashi, D. Grimaud, Y. Nojiri, J.-M. Auzende and T. Urabe	215
Deep-sea hydrothermal communities in Southwestern Pacific back-arc basins (the North Fiji and Lau Basins): Composition, microdistribution and food web D. Desbruyères, A.-M. Alayse-Danet, S. Ohta and the Scientific Parties of BIOLAU and STARMER Cruises	227
Microbial populations of hydrothermal fluid and plumes in the North Fiji Basin with reference to chemosynthesis T. Naganuma and H. Seki	243



0025-3227(199401)116:1/2;1-T

ORSTOM Documentation



010001477

O. R. S. T. O. M. Fonds Documentaire

N° 43497

Cote B ex1.